

# Analysis of the subsecond structure of X-ray and radio bursts in solar flares

© A.N. Shabalin, Yu.E. Charikov, E.M. Sklyarova

Ioffe Institute,  
194021 St. Petersburg, Russia  
e-mail: taoastronomer@gmail.com

Received May 4, 2025

Revised August 13, 2025

Accepted August 15, 2025

Studying subsecond X-ray and radio bursts (spikes) in solar flares provides insights into the temporal characteristics of magnetic reconnection and particle acceleration in the solar atmosphere. These rapid flux variations reveal the characteristic timescales of energy release processes in flares. Here, we analyzed an M2.8 flare that occurred on January 12, 2000, during which both X-ray and radio bursts were recorded. We detected bursts using an improved empirical mode decomposition technique that offers high sensitivity and a low false-positive rate. Analysis of the flare's temporal structure revealed delays between bursts in different energy bands and allowed us to estimate the plasma parameters in the emission region.

**Keywords:** solar flares, hard X-ray (HXR) emission, radio emission, sub-second bursts, particle acceleration, magnetic reconnection.

DOI: 10.61011/TP.2025.12.62486.234-25

Solar flares are the most powerful explosive processes in the Solar System, accompanied by the release of a huge amount of energy (up to  $10^{32}$  erg) in a short time (see, for example, [1]). The fundamental mechanism underlying flares is the rapid conversion of magnetic energy stored in the Sun's corona into kinetic energy of particles and thermal energy of plasma through magnetic reconnection. Hard X-ray (HXR) emission (photons with energies  $> 15-25$  keV) serves as a key diagnostic tool for studying particle acceleration mechanisms in flares. This emission arises primarily from the bremsstrahlung of accelerated electrons interacting with dense chromospheric plasma, although coronal HXR sources are also observed, albeit less frequently [1].

The time profiles of HXR emission during flares often exhibit complex structures with rapid flux variations. Of particular interest among these are sub-second bursts, or spikes, which are short (lasting from tens of milliseconds to 1–2 s) and sharp increases in HXR flux [2–5]. Spikes represent the fastest observed variations in flare X-ray emission and provide direct evidence of the fragmentation and impulsive nature of energy release and particle acceleration processes [6]. The short duration of the spikes imposes strict constraints on potential acceleration mechanisms and implies high efficiency and a high rate of energy release. Studying the temporal, spectral, and spatial characteristics of spikes, as well as their relationship with other manifestations of flare activity (e.g., radio bursts), offers a unique opportunity to investigate elementary energy release events in flare plasma and develop new methods for diagnosing its parameters [7].

The analysis of spikes presents significant challenges. Spike signals have low amplitudes and are often lost against the background noise and slowly varying components of the flare emission. Their characteristic durations are only a

few tens to hundreds of milliseconds. Traditional detection methods based on the signal exceeding a certain threshold level (e.g.,  $3\sigma$ ) may miss real events, particularly at low signal-to-noise ratios (SNR). In this study, we developed and applied an improved method for the reliable detection of sub-second spikes in noisy data. Furthermore, we investigated the characteristics of flare precursor activity and particle propagation by analyzing their temporal structure in the X-ray and radio ranges. As a case study, we considered the event of January 12, 2000. To detect sub-second bursts in observational data, we developed and applied a combined method based on the Empirical Mode Decomposition (EMD) of the time series [8]. The EMD method allows for the adaptive decomposition of a complex non-stationary signal into a set of quasi-periodic components called Intrinsic Mode Functions (IMFs). Each IMF characterizes oscillations within a specific frequency range. This capability is particularly useful for separating short-lived non-periodic spikes from quasi-periodic noise and background oscillations in the data. It enables the isolation of high-frequency signal components, against which the rapid variations characteristic of X-ray and radio spikes become more distinguishable.

The proposed combined method identifies a spike only if it satisfies the following two independent criteria simultaneously:

1) EMD-based criterion (Percentile): The original signal is decomposed into Intrinsic Mode Functions (IMFs). A spike candidate is identified if its amplitude in the high-frequency IMFs exceeds a threshold equal to the 99th percentile of the amplitude distribution of that specific mode.

2) Local variance-based criterion (Windowed  $N\sigma$ ): For the detrended signal, a spike candidate is identified if its

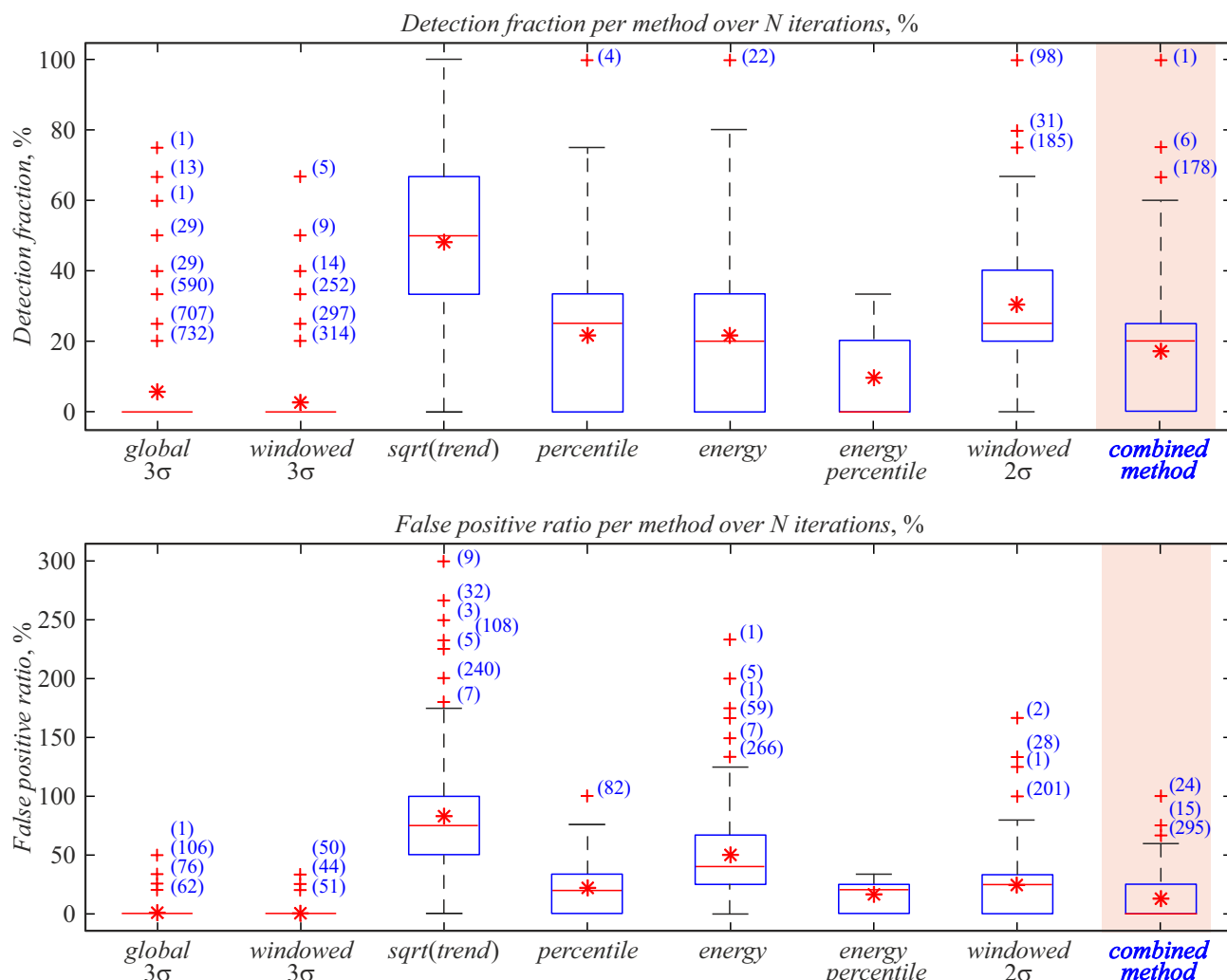


**Figure 1.** Comparison of seven spike detection methods based on the simulation of 10,000 random signals with predefined spikes and red and white noise added at  $\text{SNR} = 5 \text{ dB}$ . Upper panel — Detection Fraction. Bottom panel — False Positive Ratio. The symbols and figures on the graphs correspond to the description of the boxplot function in the MATLAB package.

amplitude exceeds  $N$  standard deviations ( $N\sigma$ ) calculated within a sliding time window. In this study, we used  $N = 2$  and a window duration of 3 s.

The final confirmation of a spike is made only if both methods detect the event simultaneously (within a tolerance comparable to the temporal resolution of the data). This approach permits the use of a lower threshold in the Windowed  $N\sigma$  ( $N = 2$ ) to increase sensitivity, while the requirement for simultaneous detection by the second, independent criterion effectively suppresses false detections.

The effectiveness of this combined method was assessed by comparing it with seven other spike detection methods:

1) Global  $3\sigma$ : A classical method that detects peaks whose amplitude in the detrended signal exceeds a level of three standard deviations ( $\sigma$ ) calculated over the entire time series.

2) Windowed  $3\sigma$ : A variation of the previous method in which the  $3\sigma$  level is calculated not for the entire signal but

within a sliding time window, allowing adaptation to local noise variations.

3)  $3\sqrt{\text{trend}}$ : A method proposed in [5], where peaks in the detrended signal are detected when they exceed the level  $3\sqrt{\text{trend}}$ , with trend representing the slowly varying component of the original signal.

4) Percentile (EMD): A method utilizing Empirical Mode Decomposition (EMD) to decompose the signal into Intrinsic Mode Functions (IMFs). Peaks are detected when the signal amplitude in one or more high-frequency IMFs exceeds a specified percentile (e.g., the 99th) of the amplitude distribution of that mode.

5) Energy Ratio (HHS): A method based on Hilbert-Huang Spectrum (HHS) analysis. The signal energy was calculated within a specific frequency range (e.g., 0.5–10 GHz). Peaks were detected when the ratio of the current energy to the threshold value (mean energy +  $N\sigma$  standard deviation of energy) exceeded 1.

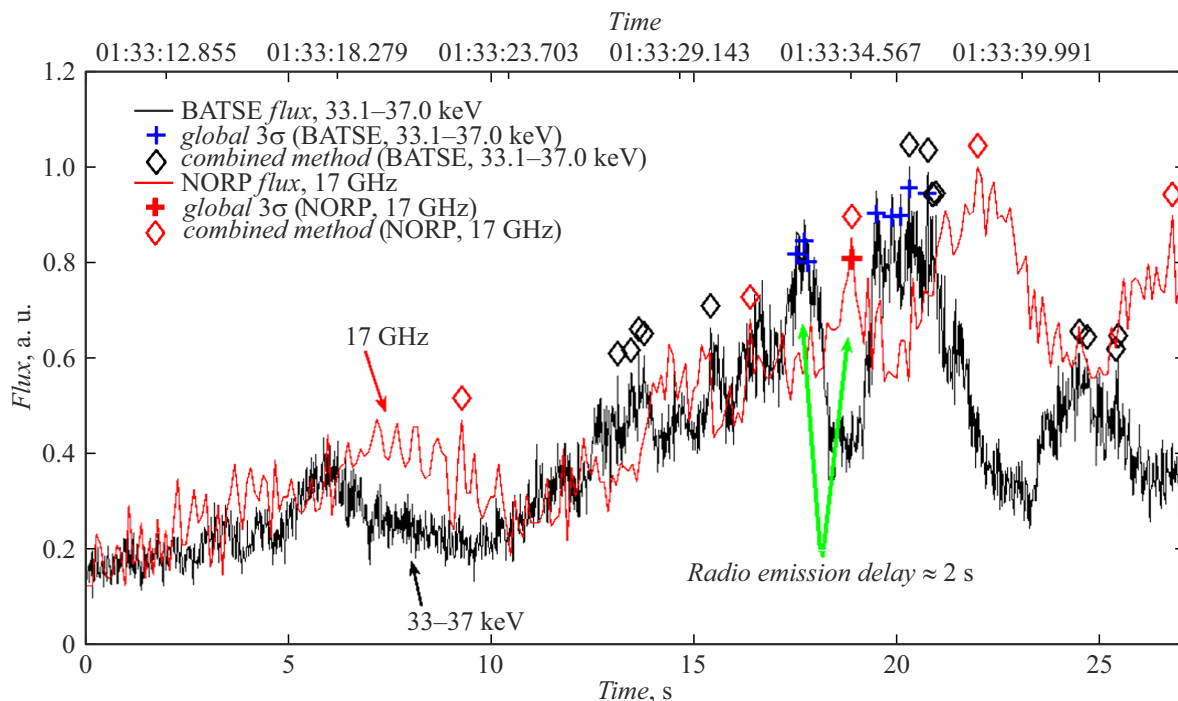


**Figure 2.** Example of detected spikes (marked with symbols) using the combined method (red diamonds for 17 GHz, black diamonds for 33–37 keV) and the global three sigma method (blue crosses for 33–37 keV, red crosses for 17 GHz) overplotted on normalized emission time profiles in the X-ray channel 33–37 keV (BATSE, black curve) and at the radio frequency 17 GHz (NORP, red curve) during the pre-flare radiation in the event on 12 January 2000. The green arrows show the characteristic delay of radio emission relative to X-ray.

6) Energy Percentile (HHS): A variation of the previous method where peaks are detected when the signal energy in a given frequency range (HHS) exceeds a threshold corresponding to a high percentile (e.g., the 99th) of the energy distribution.

7) Windowed  $N\sigma$ : A method similar to Windowed  $3\sigma$  but using a tunable multiplier  $N$  to calculate the threshold (in this study, we used  $N = 2$ ). This is one of the two methods employed in our combined approach.

The comparison results (Figure 1) show that the proposed combined method (EMD + Windowed  $N\sigma$ ) exhibits one of the highest detection probabilities for true spikes with the fewest false detections among the considered methods. The simulations were performed using 10,000 random signals with *\*a priori\**-defined spike and noise (red and white) parameters at  $\text{SNR} = 5 \text{ dB}$ . This signal-to-noise ratio was selected as the representative value. At higher  $\text{SNR}$  values ( $> 15 \text{ dB}$ ), the performance of all considered methods improved significantly, rendering their comparison less informative. Conversely, at  $\text{SNR} < 3 \text{ dB}$ , reliable detection becomes challenging for all the algorithms.

Following the development and testing of the combined method, we applied it to analyze observational data from the precursor phase of the M2.8 GOES class solar flare that occurred on January 12, 2000. We utilized data from the Burst and Transient Source Experiment (BATSE) X-ray spectrometer onboard the Compton Gamma Ray Observatory (CGRO) and from the Nobeyama Radio Polarimeters

(NORP). For the BATSE data, we analyzed X-ray emission in the 24–127 keV energy range with a temporal resolution of 16 ms. In the radio range, we used data at frequencies of 17 and 35 GHz, with a temporal resolution of 100 ms.

The analysis revealed numerous sub-second spikes in both the X-ray and radio ranges during the precursor phase of the January 12, 2000, event (Figure 2).

The main results of this study are as follows:

1. Temporal structure of spikes: The characteristic duration of the detected spikes in the X-ray and radio ranges was from 30 ms (which is close to the temporal resolution limit of the BATSE spectrometer) to several hundred ms. Such short durations correspond to the minimum detectable timescale, according to kinetic calculations [7]. This confirms that the observed spikes reflect elementary particle acceleration events and place an upper limit on the duration of these processes. The presence of numerous spikes during the precursor phase indicates the fragmentary nature of energy release even before the onset of the main flare phase.

2. Time delays: We detected a systematic time shift between groups of spikes in the X-ray and radio ranges. Radio spikes at 17 GHz lagged behind X-ray spikes in the 33–37 keV range by approximately 2 s on average (Figure 2). Such delays can be explained, for example, by trap-plus-precipitation effects in magnetic traps [9]. Another possible reason could be a two-stage acceleration process, in which the electrons responsible for radio emission (with

energies  $> 200$  keV) are accelerated later or in a different region compared to the electrons generating X-ray photons. A detailed analysis of such delays provides information on acceleration mechanisms and plasma parameters in the source.

A comparison of the results in Figure 2 illustrates the practical advantages of the proposed approach. The combined method detects a significantly larger number of spikes compared to the classical Global  $3\sigma$  method. These results highlight the importance of studying the sub-second emission structure to understand fundamental processes in flares. The detection of spikes during the precursor phase indicates that fragmentary particle acceleration processes may begin prior to the main impulsive energy release. The observed time delays between X-ray and radio spikes provide important diagnostic information regarding the geometry and physical conditions in the energy release region.

Based on the larger spike samples obtained using the developed method, future studies will include a detailed comparison of their characteristics across different energy channels, as well as a more precise temporal alignment of radio and X-ray data for the reliable identification of simultaneous events.

To quantitatively interpret the observed spike characteristics, such as their sub-second duration and the  $\sim 2$  s delay between radio and X-ray emission, future studies will focus on the numerical modeling of accelerated electron beam propagation in flare magnetic loops. The modeling aims to establish a quantitative link between the observed characteristics of X-ray and radio spikes (amplitude, duration, spectrum, and time delays) and the parameters of the flare plasma and accelerated particles. In particular, we plan to investigate the dependence of spike characteristics on the plasma density and temperature distributions along the loop, magnetic field parameters, and energy and pitch-angle distributions of accelerated electrons. Such modeling will enable the use of observed spike properties for more precise diagnostics of plasma parameters and particle acceleration characteristics in flares.

## Funding

The work was carried out within the framework of the FFUG-2024-0002 State Program.

## Conflict of interest

The authors declare that they have no conflict of interest.

## References

- [1] M.J. Aschwanden. *Physics of the Solar Corona* (Springer Berlin Heidelberg, 2006), DOI: 10.1007/3-540-30766-4
- [2] A.L. Kiplinger, B.R. Dennis, K.J. Frost, L.E. Orwig, A.G. Emslie. *Astrophys. J.*, **265**, 99 (1983). DOI: 10.1086/183966
- [3] J. Qiu, J.X. Cheng, G.J. Hurford, Y. Xu, H. Wang. *Astron. Astrophys.*, **547**, A72 (2012). DOI: 10.1051/0004-6361/201118609
- [4] J.X. Cheng, J. Qiu, M.D. Ding, H. Wang. *Astron. Astrophys.*, **547**, A73 (2012). DOI: 10.1051/0004-6361/201118608
- [5] T. Knuth, L. Glesener. *Astrophys. J.*, **903**(1), 63 (2020). DOI: 10.3847/1538-4357/abb779
- [6] A.O. Benz. *Sol. Phys.*, **96**(2), 357 (1985). DOI: 10.1007/BF00149690
- [7] Y.E. Charikov, V.I. Shuvalova, E.M. Sklyarova, A.N. Shabalin. *Geomagn. Aeron.*, **62**(8), 1085 (2022). DOI: 10.1134/S0016793222080072
- [8] G. Wang, X.Y. Chen, F.L. Qiao, Z. Wu, N.E. Huang. *Adv. Adapt. Data Anal.*, **2**(3), 277 (2010). DOI: 10.1142/S1793536910000549
- [9] M.J. Aschwanden, R.M. Bynum, T. Kosugi, H.S. Hudson, R.A. Schwartz. *Astrophys. J.*, **487**(2), 936 (1997). DOI: 10.1086/304633

Translated by A.Akhtyamov